
Optimization of the Jaccard index for image segmentation with the Lovász hinge

Maxim Berman
ESAT-PSI
KU Leuven
Kasteelpark Arenberg 10
3001 Leuven, Belgium
maxim.berman@esat.kuleuven.be

Matthew B. Blaschko
ESAT-PSI
KU Leuven
Kasteelpark Arenberg 10
3001 Leuven, Belgium
matthew.blaschko@esat.kuleuven.be

Abstract

The Jaccard loss, commonly referred to as the intersection-over-union loss, is commonly employed in the evaluation of segmentation quality due to its better perceptual quality and scale invariance, which lends appropriate relevance to small objects compared with per-pixel losses. We present a method for direct optimization of the per-image intersection-over-union loss in neural networks, in the context of semantic image segmentation, based on a convex surrogate: the Lovász hinge. The loss is shown to perform better with respect to the Jaccard index measure than other losses traditionally used in the context of semantic segmentation; such as cross-entropy. We develop a specialized optimization method, based on an efficient computation of the proximal operator of the Lovász hinge, yielding reliably faster and more stable optimization than alternatives. We demonstrate the effectiveness of the method by showing substantially improved intersection-over-union segmentation scores on the Pascal VOC dataset using a state-of-the-art deep learning segmentation architecture.

1 Introduction

We consider the task of binary image segmentation, where each pixel of a given image has to be classified into a foreground or a background class. A common performance measure for evaluating segmentation masks is the Jaccard index, which, given a ground truth labeling \mathbf{y}^* and a labeling to be evaluated $\tilde{\mathbf{y}}$ is defined as

$$J(\mathbf{y}^*, \tilde{\mathbf{y}}) = \frac{|\mathbf{y}^* \cap \tilde{\mathbf{y}}|}{|\mathbf{y}^* \cup \tilde{\mathbf{y}}|}, \quad (1)$$

with the convention that $J(\mathbf{0}, \mathbf{0}) = 0$. A corresponding loss function to be employed in empirical risk minimization is $\Delta_J(\mathbf{y}^*, \tilde{\mathbf{y}}) = 1 - J(\mathbf{y}^*, \tilde{\mathbf{y}})$. We develop here a method for optimizing the performance of a discriminatively trained segmentation system with respect to the Jaccard index, sometimes call the intersection-over-union score. We demonstrate that a piecewise linear convex surrogate to the Jaccard loss based on the Lovász extension of a set function yields consistent improvement of segmentation as measured by the Jaccard index, and we develop a proximal gradient based method for its fast and stable optimization.

Although the Jaccard index is often used globally, over every pixel of the evaluated segmentation dataset, it can also be used independently on each image. Using the per-image Jaccard index is known to have better perceptual accuracy by reducing the bias towards large instances of the object classes in the dataset [6]. Due to these favorable properties, and the empirical risk minimization principle of optimizing the loss of interest at training time [20], optimization of the Jaccard loss during training has been frequently considered in the literature. However, in contrast to the present submission,

existing methods all have significant shortcomings that do not allow plug-and-play application to a wide range of learning architectures.

[17] provides a Bayesian framework for optimization of the Jaccard index, but uses “a statistical approximation to the objective function, as well as an approximate algorithm based on parametric linear programming.” [2] optimizes IoU by selecting among a number of candidate segmentations, not by optimizing segmentation algorithms with respect to the loss directly. [3] optimize the Jaccard loss in a structured output SVM, but are only able to do so by using a branch-and-bound optimization over bounding boxes and not full segmentations.

Alternative approaches train binary classifiers, but on data that are sampled to capture high Jaccard index. [4, 11] use IoU and related overlap measures to define training sets for binary classifiers in complex multi-stage training strategies. Such sampling based approaches will clearly introduce suboptimality in the empirical risk approximation and do not lend themselves to convenient modular application in a deep learning setting.

Still other recent high-impact research has highlighted the need for optimization of the Jaccard index, but resort to binary training as a proxy, presumably for lack of a convenient and flexible method of directly optimizing the loss of interest. [15] train with logistic loss and test with the Jaccard index. The paper introducing the highly influential OverFeat network specifically addresses the shortcoming in the discussion section [18]: “We are using ℓ_2 loss, rather than directly optimizing the intersection-over-union (IOU) criterion on which performance is measured. Swapping the loss to this should be possible...” However, this is left to future work. In this paper, we develop the necessary plug-and-play loss layer to enable flexible direct minimization of the Jaccard loss in a deep learning setting, while demonstrating its applicability to training a state-of-the-art image segmentation network.

Our approach in this paper is based on the recent development of a general strategy for generating convex surrogates to submodular loss functions, the Lovász hinge [22]. Based on the result that the Jaccard loss is submodular [21, Proposition 11], this strategy is directly applicable. [21] have demonstrated optimization of the Jaccard loss on a shallow image classification task based on a cutting plane approach in a batch optimization setting. In this work, we (i) apply the Lovász hinge with Jaccard loss to the problem of image segmentation rather than image classification, (ii) demonstrate instability of state-of-the-art stochastic gradient descent approaches due to the non-differentiability of the piecewise linear loss function, (iii) develop a proximal gradient strategy to efficiently and stably optimize a deep network with respect to this surrogate, and (iv) demonstrate a substantial and consistent improvement in performance measured by the Jaccard index in a state-of-the-art deep learning based segmentation system.

2 Lovász hinge

In order to optimize the Jaccard index in a continuous optimization framework, we use the Lovász hinge, a tight convex surrogate to submodular losses [22]. The extension is based on submodular analysis of set functions, where the set function maps from a set of mispredictions to the reals [22, Equation (6)]. Two properties of set functions are of particular interest in this work, submodularity and monotonicity.

Definition 1 (Submodularity [8]). *A set function $F : \mathcal{P}(V) \rightarrow \mathbb{R}$ on some base set V is submodular if for all $A, B \subseteq V$*

$$F(A) + F(B) \geq F(A \cup B) + F(A \cap B) \quad (2)$$

Definition 2 (Monotonic set function [8]). *A set function $F : \mathcal{P}(V) \rightarrow \mathbb{R}$ is increasing if for all subsets $A \subset V$ and $x \in V \setminus A$, $F(A) \leq F(A \cup \{x\})$.*

Given an increasing submodular set function $F : \mathcal{P}(V) \rightarrow \mathbb{R}$ with $|V| = d$, the Lovász hinge extension is defined as

$$\tilde{F}(\gamma \in \mathbb{R}^d) = \sum_{p=0}^{d-1} (\gamma_{\pi(p)})_+ (F(\{\pi_0, \dots, \pi_p\}) - F(\{\pi_0, \dots, \pi_{p-1}\})) \quad (3)$$

with $(x)_+ = \max(x, 0)$ and π is the permutation ordering the margins γ in decreasing order. The extension is convex, piecewise-linear, tight in the case of increasing submodular losses, as it is

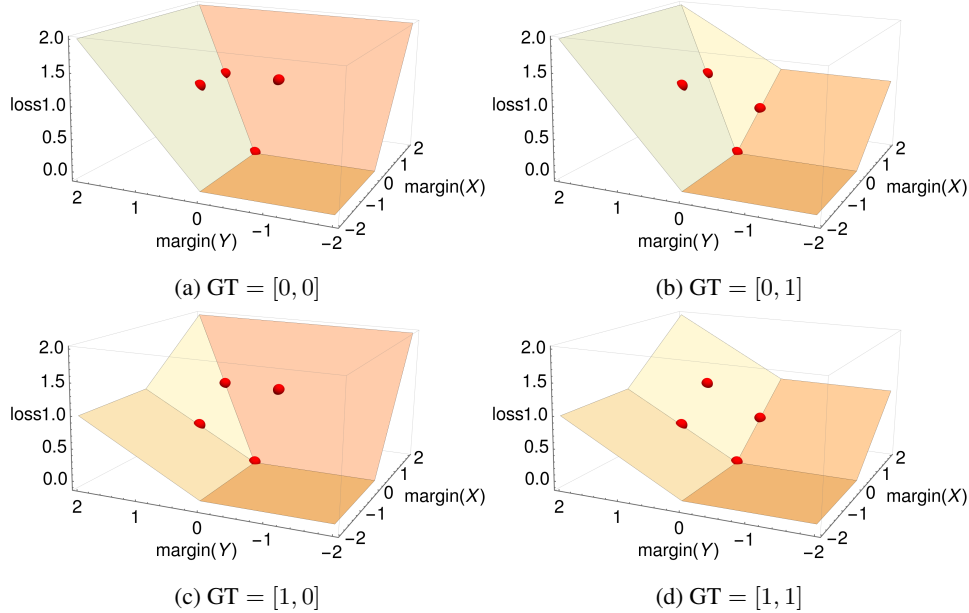


Figure 1: Lovász hinge in the case of two pixel predictions for the four possible ground truths GT. The red dots indicate the values of the discrete Jaccard index.

built on the Lovász extension for submodular set functions [16]. Moreover, by the use of positive thresholding, extension (3) reduces to the standard hinge loss in the case of a single prediction.

The Lovász hinge is only applicable to loss functions that are submodular in the set of mispredictions [22].

Theorem 1. (Submodularity of the Jaccard loss [21, Proposition 11]) *The Jaccard loss is submodular and increasing in the set of mispredictions and the application of the Lovász hinge is therefore convex and well-defined.*

Figure 1 illustrates the extension of the Jaccard loss in the case of two pixels.

Naïve computation of Equation (3) can be achieved by sorting the elements of γ in $\mathcal{O}(d \log d)$ time and then calling F $\mathcal{O}(d)$ times. However, if we compute F by Equation (1), each call will cost $\mathcal{O}(d)$. As π is known in advance, we may simply keep track of the cumulative number of false positives and negatives in $\{\pi_0, \dots, \pi_p\}$ for increasing p yielding an amortized $\mathcal{O}(1)$ cost per evaluation of F (cf. [21, Equation (43)]). As we are explicitly computing each of the summands of Equation (3), this procedure yields the loss gradient at the same computational cost. This is a powerful result implying that a tight surrogate function for the Jaccard loss is available and computable in $\mathcal{O}(d \log d)$ time.

In practice, the most effective function classes for image segmentation are currently defined by deep neural networks [9]. These networks are typically trained using variants of stochastic gradient descent, which may have problems with instability while optimizing non-differentiable objectives. Indeed, we have observed such instability when directly applying the Lovász hinge to train deep network architectures. We therefore analyze the applicability of (variants of) the proximal gradient algorithm for optimization of a risk functional based on the Lovász hinge.

3 Proximal gradient algorithm

Definition 3 (Proximal operator). *The proximal operator of a function f with a regularization parameter λ is*

$$\text{prox}_{f,\lambda}(x) = \arg \min_u f(u) + \frac{\lambda}{2} \|u - x\|^2 \quad (4)$$

For computing the proximal operator of the Lovász hinge of increasing submodular functions, we introduce Algorithm 1, which follows a greedy path.

Algorithm 1 Computation of $\text{prox}_{\tilde{F},\lambda}(\gamma)$

Input: Current margins γ, F, λ

Output: $\gamma^* = \text{prox}_{\tilde{F},\lambda}(\gamma)$

```
1:  $\mathbf{v}^0, \pi \leftarrow$  decreasing ordering of  $\gamma$  and permutation
2:  $\mathbf{v} \leftarrow \mathbf{v}^0$ 
3:  $\mathbf{g} \leftarrow \text{grad } \tilde{F}(v)$  (as a function of the sorted margins)
4:  $\mathbf{E} \leftarrow \{\text{constraint } g_i = g_{i+1} = \dots = g_{i+p} \text{ for each equality } v_i = v_{i+1} = \dots = v_{i+p}\}$ 
5:  $\mathbf{c}_z \leftarrow$  constraint  $g_{z+1} = \dots = g_d$  for  $z$  minimal index such that  $\hat{\gamma}_z < 0$ 
6: finished  $\leftarrow$  False
7: while not finished do
8:   if  $\mathbf{g} = \mathbf{0}$  : break
9:    $\mathbf{g} \leftarrow \text{proj}_{\mathbf{E} \cup \{\mathbf{c}_z\}} \mathbf{g}$ 
10:   $\mathbf{v}_{\text{next}} \leftarrow$  projection of  $\mathbf{v}$  on the closest edge of  $\tilde{F}$  in the direction  $\mathbf{g}$ 
11:  stop  $\leftarrow 1/\lambda + \langle \mathbf{v} - \mathbf{v}^0, \mathbf{g} \rangle / \langle \mathbf{g}, \mathbf{g} \rangle$ 
12:  if stop  $< \|\mathbf{v}_{\text{next}} - \mathbf{v}\|$  then
13:     $\mathbf{v} \leftarrow \mathbf{v} + \text{stop} \cdot \mathbf{g}$ 
14:    finished  $\leftarrow$  True
15:  else
16:     $\mathbf{v} \leftarrow \mathbf{v}_{\text{next}}$ 
17:    Add corresponding new constraint to  $\mathbf{E}$  or update  $\mathbf{c}_z$ 
18:  end if
19: end while
20: return  $\gamma^* = \mathbf{v}[\pi^{-1}]$ 
```

Iterative application of the proximal operator with an appropriately decreasing schedule of $\{\lambda_t\}_{0 \leq t \leq \infty}$ leads to convergence to a local minimum analogously to gradient descent. Furthermore, it is straightforward to show that, given an appropriately chosen schedule of λ parameters, the proximal gradient algorithm will converge at least as fast as gradient descent.

Proposition 1. *Given a gradient descent parameter η , $x_{t+1} = x_t - \eta \nabla \tilde{F}(x_t)$, there exists a set of descent parameters $\{\lambda_t\}_{0 \leq t \leq \infty}$ such that (i) the step size of the proximal operator is equivalent to gradient descent and (ii) $\text{prox}_{\tilde{F}}(x_t) \leq x_t - \eta \nabla \tilde{F}(x_t)$.*

Proof. Starting with claim (i), we note that the proximal operator is the Lagrangian of the constrained optimization problem $\arg \min_u \tilde{F}(u)$ s.t. $\|x - u\|^2 \leq R$ for some $R \in \mathbb{R}_{++}$, and we may therefore consider λ_t such that $R_t = \|\eta \nabla \tilde{F}(x_t)\|^2$, where $\{x_t\}_{0 \leq t \leq \infty}$ is the sequence of values visited in gradient descent.

Claim (ii) follows directly from the definition of the proximal operator as the minimization of $\tilde{F}(u)$ within a ball of radius R_t around x_t must be at least as small as the value at the gradient descent direction. \square

It is straightforward to convert a gradient descent step size schedule to an equivalent proximal gradient schedule of λ_t values such that, were the objective linear, the two algorithms would be equivalent. Indeed, the proximal gradient algorithm applied to a piecewise linear objective only differs from gradient descent at the boundaries between linear pieces, in which case it converges in a strictly smaller number of steps than gradient descent.

We optimize a deep neural network architecture by a modified backpropagation algorithm in which the gradient direction with respect to the loss layer is given by the direction of the empirical difference $x_t - \text{prox}_{\tilde{F}}(x_t)$. We note that this modification to the standard gradient computation is compatible with popular optimization strategies such as Adam [13]. In initial experiments using the true gradient rather than that based on the proximal operator, we found that the use of momentum led to faster empirical convergence than Adam, and we therefore have based our subsequent comparison and empirical results on optimization with momentum. We show here that these momentum terms still do not lead in practice to as efficient update directions as those defined by the proximal operator.

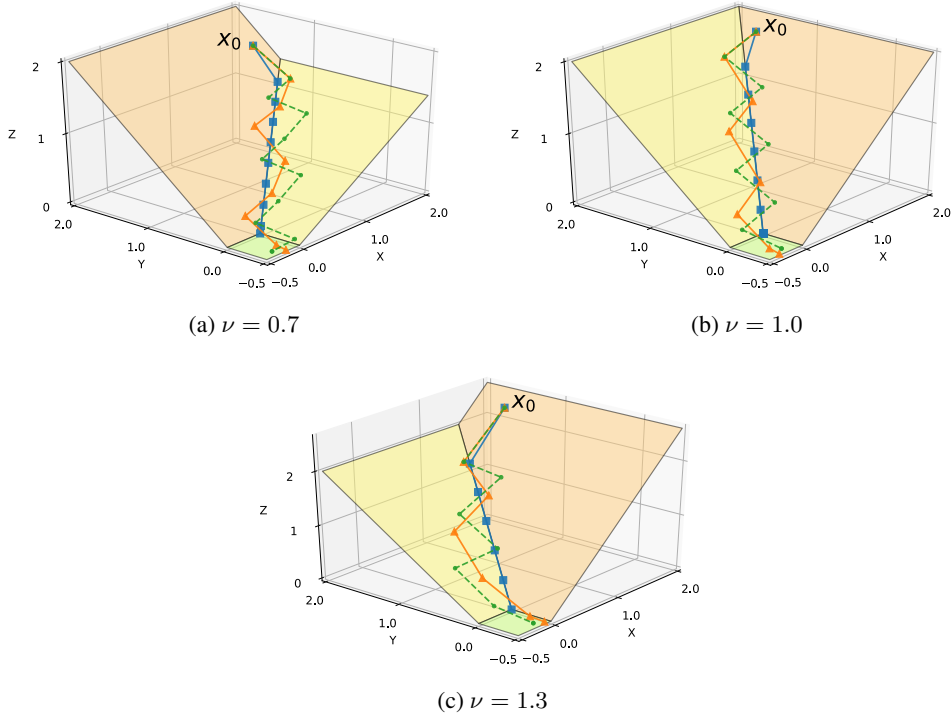


Figure 2: Optimization behavior of the piecewise-linear surface defined in Equation 7: gradient descent (green, dashed) and momentum (orange, plain) oscillate around the edge, while the proximal algorithm (green) finds the optimal descent direction.

Definition 4 (Momentum [19]). *Gradient descent with momentum is achieved with the following update rules*

$$v_{t+1} = \alpha v_t + \nabla \tilde{F}(x_t) \quad (5)$$

$$x_{t+1} = x_t - \eta v_{t+1}, \quad (6)$$

where η is the gradient descent parameter and $\alpha \in [0, 1]$ is the momentum coefficient.

Unrolling this recursion shows that momentum gives an exponentially decaying weighted average of previous gradient values, and setting $\alpha = 0$ recovers classical gradient descent.

4 Experiments

4.1 Synthetic experiments

Figure 2 shows the behavior of gradient descent with momentum on the problem

$$\min_{x \in \mathbb{R}^2} \max \left(0, \left\langle x, \begin{pmatrix} \nu \\ 0 \end{pmatrix} \right\rangle, \left\langle x, \begin{pmatrix} 0 \\ 1 \end{pmatrix} \right\rangle \right), \quad (7)$$

where ν is a positive scalar that allows us to adjust the relative scale of the gradients on either side of the boundary between the pieces. In all cases, the momentum oscillates around piecewise-linear edges, and in Figure 2c, we see that traversing to a piece of the loss surface with very different slope can lead to multiple steps away from the boundary before returning to a steeper descent direction. By contrast, the proximal algorithm immediately determines the optimal descent direction.

We demonstrate the relevance of the use of the Jaccard loss for binary segmentation using a synthetic binary image segmentation experiment. We generate $N = 10$ binary images x_1, \dots, x_{10} of size 50×50 representing circles of various radius, and extract for each pixel p a single feature using a unit

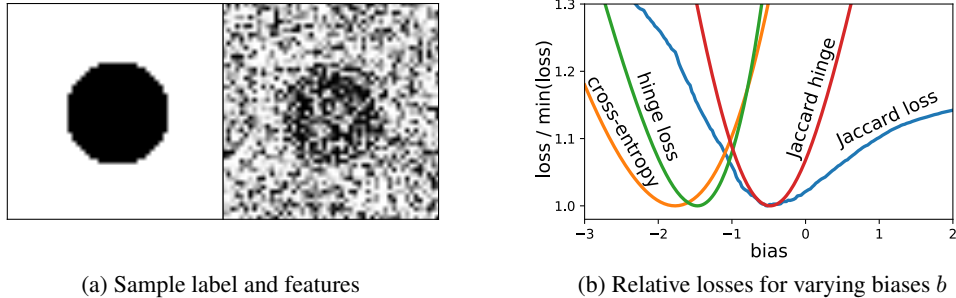


Figure 3: Synthetic model studied in 4.1 and loss objectives.

variance Gaussian perturbation of the ground truth, $f_p \sim \mathcal{N}(\epsilon, 1)$ where $\epsilon = 1/2$ for the foreground and $-1/2$ for the background, as pictured in Figure 3a.

The model we consider classifies pixels in the foreground class for $f_p > -b$; we consider the learning of the bias term b . An exhaustive search, illustrated by Figure 3b, shows that among the losses considered, only the Jaccard hinge loss function efficiently captures the absolute minimum of the Jaccard loss.

4.2 Binary segmentation on Pascal VOC

We base our experiments on the DeeplabV2 semantic segmentation network [5]. The network uses a Resnet-101 [12] based architecture, re-purposed for image segmentation, notably using dilated (or *trous*) convolutions. We use the initialization weights provided by the authors. These weights were pre-trained on MS-COCO [14] using cross-entropy loss and weight decay. We further fine-tune these weights on a segmentation dataset made of Pascal VOC 2012 training images [7] and the extra images provided by [10]), as is common in recent semantic image segmentation applications. We perform an initial fine-tuning of the weights using cross-entropy loss alone jointly on the 21 classes of Pascal VOC (including the background class). This constitutes our basis network; it obtains a validation mIoU of 76.1% on the VOC 2012 validation set when evaluated in a multi-scale setting, down to 74.9% when evaluated on a single scale. In order to evaluate our method in a purely feed-forward setting trainable end-to-end, we do not apply the Gaussian CRF post-processing step used in [5].

We then turn to binary segmentation by selecting one particular class and finetuning the output of the network corresponding to the selected class. In order to consider a realistic binary segmentation setting, we choose to sample the validation set such that half of the images contain at least one pixel of the selected class. The training set is similarly trained by biasing the selection of the training images of Pascal VOC such that on average, half of the sampled images contain the class at hand. The training is done on random crops of size 321×321 extracted from the training set, with random horizontal flipping.

In this setting, our experiments revolve around the choice of the loss for this binary segmentation task. We do a fine-tuning of 2 epoch iterations; we choose a learning rate of 0.0005 common to all losses, and reduce it to 0.0001 after 1 epoch.

Performance of the surrogate We show here the impact of directly optimizing the Jaccard Hinge on the image-iou measure. Table 1 shows the measures of the losses considered after a training with different loss objectives. Evidently, training with a particular loss leads generally to a better objective value of this loss on the validation set. Moreover, we see that the Jaccard hinge acts as a good surrogate of the discrete image-iou, leading to a better validation accuracy for this measure.

Figure 4 compares resulting segmentations after optimization of the three losses considered. We see that the Jaccard loss tends to fill gaps in segmentation, recover small objects, and lead to a more sensible segmentation globally.

Optimization study We investigate the choice of the optimization in terms of empirical convergence rates on the validation data. We first evaluate the use of varying optimization strategies for the

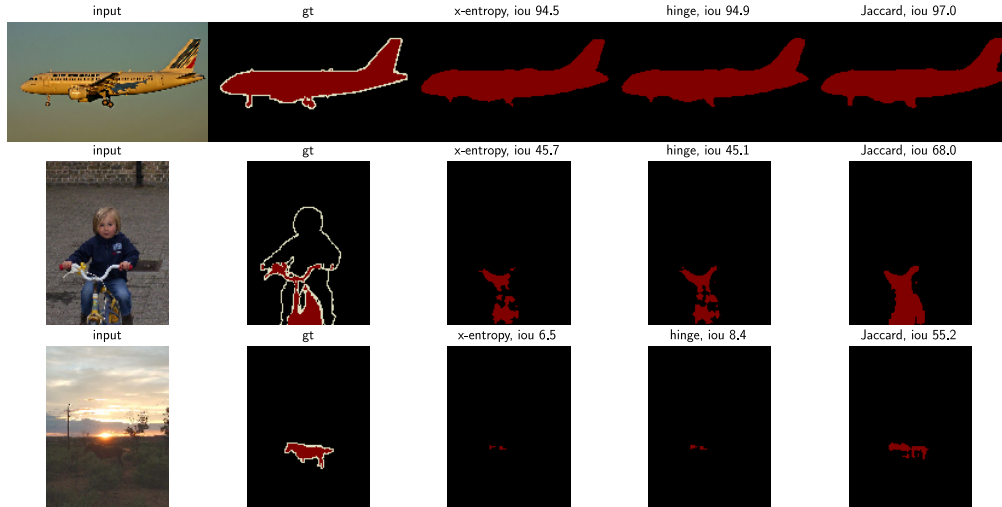


Figure 4: Example segmentations trained with different losses and associated iou scores on Pascal VOC.

Table 1: Losses measured on our validation set of 5 categories of Pascal VOC, after a training with cross-entropy loss (**x**), hinge-loss (**h**), and Jaccard-hinge (**j**). **b** indicates the performance of the basis network, trained for all categories.

<i>training</i>	aeroplane				bicycle			
	b	x	h	j	b	x	h	j
x-entropy, $\cdot 10^{-2}$		2.8	3.3	4.1		12.3	11.0	11.3
hinge, $\cdot 10^{-2}$		2.9	2.6	2.8		14.8	12.1	11.5
Jacc-Hinge, $\cdot 10^{-1}$		3.8	3.6	2.8		13.8	12.0	9.2
IoU, %	86.2	88.6	87.7	89.6	63.2	61.2	58.7	66.3

dog				horse				motorbike			
b	x	h	j	b	x	h	j	b	x	h	j
	5.7	6.0	6.3		5.2	6.2	6.5		6.2	6.6	7.2
	6.3	5.8	5.8		5.7	5.3	5.8		7.0	6.4	6.8
	5.6	5.0	3.4		6.0	5.7	4.6		5.1	4.8	3.7
83.8	82.1	81.7	87.6	82.4	82.1	79.1	84.8	83.8	82.6	82.8	85.4

last layer of the network in Figure 5. Figure 6 shows the convergence of the validation loss across the optimization of different loss functions.

5 Discussion and Conclusions

In this work, we have demonstrated the most flexible approach to optimization of the Jaccard loss for image segmentation present in the literature. Our proposed method can be flexibly applied to a large number of function classes for segmentation, and we have demonstrated their effectiveness on a state-of-the-art deep network architecture, substantially improving accuracies on the benchmark Pascal VOC dataset simply by optimizing the correct loss during training. Improvement in accuracies can be quite substantial, e.g. on the *dog* class, we show an improvement in IoU from 82.1 to 87.6, a more than 25% reduction in residual error. Qualitatively, we see greatly improved segmentation quality, in particular on small objects, while large objects tend to have consistent but smaller improvement in accuracy.

Convergence rates demonstrate that the proposed optimization framework, based on an adaptation of proximal gradient methods, yields highly efficient optimization. Indeed Figure 6 shows that the

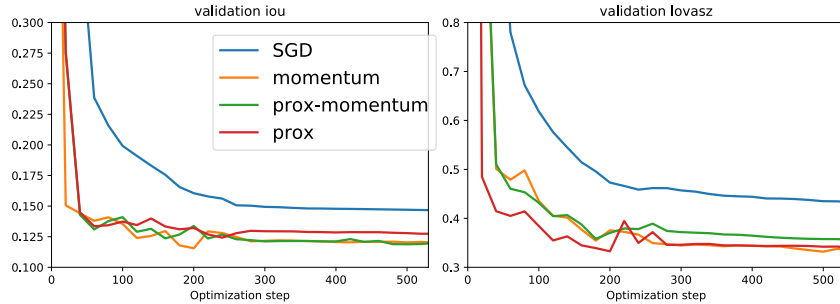


Figure 5: Jaccard loss optimization with different optimization methods.

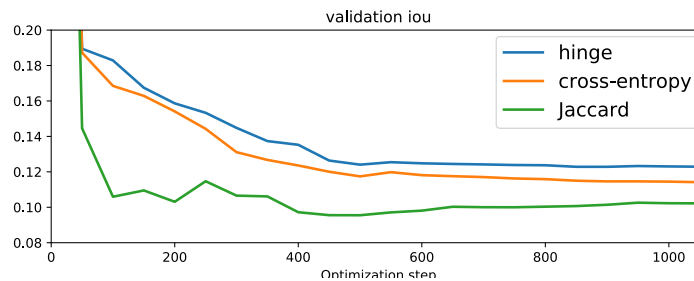


Figure 6: Evolution of the validation IoU during the course of the optimization with the different losses considered.

proximal optimization strategy applied to the Jaccard loss converges much faster than state-of-the-art optimization on cross-entropy loss.

This work shows that the Lovász hinge is a suitable loss for optimization of submodular measures in a continuous optimization setting, such as the Jaccard index. Using this approach, we demonstrated the relevance of directly optimizing the intersection over union in segmentation datasets. We also presented a specialized optimization algorithm suited to the optimization of the Lovász hinge loss. Further work include the extension of our approach to a multi-class segmentation setting, the application of the approach to different tasks and losses exhibiting submodularity, and a generalization of the stochastic proximal optimization algorithm presented here to more general settings.

The code released on <https://github.com/bermanmaxim/jaccardSegment> presents an implementation of the Jaccard Hinge loss and adapted proximal optimization method studied in this article, with replication of the Pascal VOC experiments, in the PyTorch [1] deep learning framework.

Acknowledgements

This work is partially funded by Internal Funds KU Leuven and FP7-MC-CIG 334380. We acknowledge support from the Research Foundation - Flanders (FWO) through project number G0A2716N.

References

- [1] PyTorch: Tensors and dynamic neural networks in python with strong gpu acceleration. <http://pytorch.org/>.
- [2] F. Ahmed, D. Tarlow, and D. Batra. Optimizing expected intersection-over-union with candidate-constrained crfs. In *The IEEE International Conference on Computer Vision (ICCV)*, December 2015.
- [3] M. B. Blaschko and C. H. Lampert. Learning to localize objects with structured output regression. In D. Forsyth, P. Torr, and A. Zisserman, editors, *Computer Vision – ECCV*, volume 5302 of *Lecture Notes in Computer Science*, pages 2–15. Springer, 2008.

- [4] L. Bourdev, S. Maji, T. Brox, and J. Malik. Detecting people using mutually consistent poselet activations. In K. Daniilidis, P. Maragos, and N. Paragios, editors, *European Conference on Computer Vision, Part VI*, pages 168–181. Springer, 2010.
- [5] L.-C. Chen, G. Papandreou, I. Kokkinos, K. Murphy, and A. L. Yuille. Deeplab: Semantic image segmentation with deep convolutional nets, atrous convolution, and fully connected crfs. *arXiv:1606.00915*, 2016.
- [6] G. Csurka, D. Larlus, F. Perronnin, and F. Meylan. What is a good evaluation measure for semantic segmentation? In *Proceedings of the British Machine Vision Conference*, volume 27, 2013.
- [7] M. Everingham, L. Van Gool, C. K. I. Williams, J. Winn, and A. Zisserman. The PASCAL Visual Object Classes Challenge 2012 (VOC2012) Results. <http://www.pascal-network.org/challenges/VOC/voc2012/workshop/index.html>.
- [8] S. Fujishige. *Submodular Functions and Optimization*. Annals of Discrete Mathematics. Elsevier Science, 2005.
- [9] I. Goodfellow, Y. Bengio, and A. Courville. *Deep Learning*. MIT Press, 2016.
- [10] B. Hariharan, P. Arbelaez, L. Bourdev, S. Maji, and J. Malik. Semantic contours from inverse detectors. In *International Conference on Computer Vision (ICCV)*, 2011.
- [11] B. Hariharan, P. Arbeláez, R. Girshick, and J. Malik. *Simultaneous Detection and Segmentation*, pages 297–312. 2014.
- [12] K. He, X. Zhang, S. Ren, and J. Sun. Deep residual learning for image recognition. In *Proceedings of the IEEE Conference on Computer Vision and Pattern Recognition*, pages 770–778, 2016.
- [13] D. P. Kingma and J. Ba. Adam: A method for stochastic optimization. In *Proceedings of the 3rd International Conference on Learning Representations (ICLR)*, 2014.
- [14] T.-Y. Lin, M. Maire, S. Belongie, J. Hays, P. Perona, D. Ramanan, P. Dollár, and C. L. Zitnick. Microsoft coco: Common objects in context. In *European Conference on Computer Vision*, pages 740–755. Springer, 2014.
- [15] J. Long, E. Shelhamer, and T. Darrell. Fully convolutional networks for semantic segmentation. In *The IEEE Conference on Computer Vision and Pattern Recognition (CVPR)*, June 2015.
- [16] L. Lovász. Submodular functions and convexity. In *Mathematical Programming The State of the Art*, pages 235–257. Springer, 1983.
- [17] S. Nowozin. Optimal decisions from probabilistic models: The intersection-over-union case. In *The IEEE Conference on Computer Vision and Pattern Recognition (CVPR)*, June 2014.
- [18] P. Sermanet, D. Eigen, X. Zhang, M. Mathieu, R. Fergus, and Y. LeCun. Overfeat: Integrated recognition, localization and detection using convolutional networks. *CoRR*, abs/1312.6229, 2013. URL <http://arxiv.org/abs/1312.6229>.
- [19] I. Sutskever, J. Martens, G. Dahl, and G. Hinton. On the importance of initialization and momentum in deep learning. In *Proceedings of the 30th International Conference on International Conference on Machine Learning*, pages III–1139–1147, 2013.
- [20] V. N. Vapnik. *The Nature of Statistical Learning Theory*. Springer, 1995.
- [21] J. Yu and M. B. Blaschko. The Lovász hinge: A convex surrogate for submodular losses. 2015. *arXiv:1512.07797*.
- [22] J. Yu and M. B. Blaschko. Learning submodular losses with the Lovász hinge. In *Proceedings of the 32nd International Conference on Machine Learning*, volume 37 of *Journal of Machine Learning Research: W&CP*, pages 1623—1631, Lille, France, 2015.